Additive Manufacturing of Embedded Thermocouples in WC-Co Cutting Tools for Cutting Temperature Measurement

Bruno Guimarães, Filipe S. Silva
Center for MicroElectroMechanical Systems (CMEMS-UMinho), University of Minho, Campus de Azurém, 4800-058 Guimarães, Portugal

Cristina M. Fernandes, Daniel Figueiredo
Palbit S.A., P.O. Box 4, 3854-908 Branca, Portugal

Georgina Miranda
CICECO, Aveiro Institute of Materials, Department of Materials and Ceramic Engineering, University of Aveiro, 3810-193 Aveiro, Portugal

ABSTRACT

During machining processes, a large amount of heat is generated due to deformation of the material and friction of the chip along the surface of the tool, especially in the cutting zone. This high temperature strongly influences tribological phenomena and adhesion, tool wear, tool life, workpiece surface integrity and quality, chip formation mechanisms and contribute to the thermal deformation of the cutting tool, leading to high operating costs and reduction of the end product quality. In this sense, being able to assess the cutting temperature in real time, at various points of the cutting tool during machining processes, is of utmost importance to effectively optimize cutting parameters and the cutting fluid flow adequately, for minimizing heat generation, temperature and consequently wear, allowing to increase tool life.

This work proposes the fabrication of embedded additively manufactured type K and type N thermocouples by laser powder bed fusion for real time cutting temperature measurement. Processing parameters optimization was performed to obtain a dense and continuous thermocouple with no significant defects and the additively manufactured thermocouples were tested in comparison to a conventional thermocouple. The obtained results show that this approach is effective to produce embedded thermocouples in WC-Co cutting tools capable of measuring cutting temperature, which will allow a real time optimization of the cutting parameters, namely cutting speed, feed and depth of cut, during in-service time, thus enhancing tool performance and life.

INTRODUCTION

During machining processes, a large amount of heat is generated, being estimated that approximately 90% of the mechanical work applied to the workpiece is transformed in thermal energy, due to deformation of the material and friction of the chip along the surface of the tool, especially in the cutting zone [1,2]. This high temperature strongly influences tribological phenomena and adhesion, tool wear, tool life, workpiece surface integrity and quality, chip formation mechanisms and contribute to the thermal deformation of the cutting tool, leading to high operating costs and reduction of the end product quality [3–5]. In this sense, the ability to measure cutting temperature in real time, at various points of the cutting tool during machining processes, is of utmost importance to effectively optimize cutting parameters and the cutting

fluid flow adequately, for minimizing heat generation, temperature and consequently wear, allowing to increase tool life [6,7].

Several cutting temperature measurement methods were developed over the years, such as embedded, tool-work, traverse, single-wire and thin-film thermocouple, thermal paints, fine powders, PVD coatings, metallographic methods, infrared pyrometry, and infrared thermography [2,8], but due to the movement of the cutting tool or workpiece, chip obstruction on the rake face, small contact areas involved, and large wear mechanisms, none can be considered flawless and able to provide accurate results in all situations [9].

Thermocouples have become the standard method for cost-effective temperature measurement, due to their low cost, robust nature, simplicity to mount and capability to operate over a wide temperature range [4,10,11]. The best known and widely used thermocouple in industry for measuring medium and high temperatures is the type K thermocouple (chromel-alumel), due to its good oxidation resistance, extended temperature range (-200 °C up to 1100 °C), emf temperature curve reasonably linear and sensitivity of 41 μV/°C [12,13]. Type N thermocouple (nicrosil-nisil) is the most recent among the different thermocouple types that use base metals and is increasingly being more used in industry, slowly becoming dominant over type K, because it offers higher thermoelectric stability and better oxidation resistance than other thermocouple types [14,15]. This thermocouple is ideally suited for temperature measurements in air up to 1200 °C, being able to withstand slightly higher temperatures in vacuum or controlled atmospheres. Its sensitivity of 39 μV/°C at 900 °C is slightly lower than type K thermocouple [12].

Laser powder bed fusion (LPBF) is an additive manufacturing technology that uses a laser to selectively melt layers of powder, to produce objects layer by layer from a 3D model data. This technology has the ability to produce high quality and high precision complex components with unmatched degrees of freedom [16–18]. Multi-material LPBF combines the advantages of traditional LPBF with the ability to create multi-material 3D components, providing new opportunities for the development of components with a high level of functionality and varying properties, due to distinct materials being placed in different locations in a single component [19,20].

The thermocouple working principle, junction of two dissimilar materials, allows taking advantage of the multi-material LPBF technology, for producing additively manufacture temperature sensors. In this sense, this work proposes the fabrication of embedded additively manufactured type K and type N thermocouples by laser powder bed fusion for real time cutting temperature measurement. Processing parameters optimization was performed to obtain a dense and continuous thermocouple with no significant defects and the additively manufactured thermocouples were tested in comparison to a conventional thermocouple. Prior to thermocouple embedding, laser surface modification parameters optimization was performed to obtain a micro-groove with suitable dimensions for embedding the additively manufactured thermocouple.

MATERIALS AND METHODS

Micro-grooves production

WC-10wt.%Co is one of the most used compositions for cutting tools, due to its inherent high hardness and toughness, and wear resistance [21,22]. For this reason, WC-10wt.%Co substrates were selected for being embedded with the additively manufactured type K and type N thermocouples. For this, first the substrates were surface modified with an Nd:YVO4 fibre laser (wavelength of 1064 nm) with a maximum working power of 30 W, a laser spot size of 10 μm, a pulse width of approximately 10 μs, to obtain grooves with suitable dimensions, 240 μm width and 120 μm depth, for subsequent thermocouples alloys powder filling with particle size below 50 μm and production of embedded thermocouples by LPBF.

In order to assess the optimum laser parameters, several different combinations of parameters were tested, as presented in Table 1. To achieve the desired groove width, multiple scan lines with a line spacing of 10 µm between them were used, until the desired width was reached. In Figure 1 is depicted a schematic representation of the process used for micro-grooves production. The influence of the different laser parameters combinations on the topography of the produced micro-grooves was evaluated by Scanning Electron Microscopy (SEM). A SEM - JEOL JSM-6010L equipment was used for this analysis.

During laser processing, a jet of air was used to remove the debris produced and then, all samples were ultrasonically cleaned in isopropyl alcohol for 5 min and airdried to remove any remaining debris and contaminants resulting from the process.

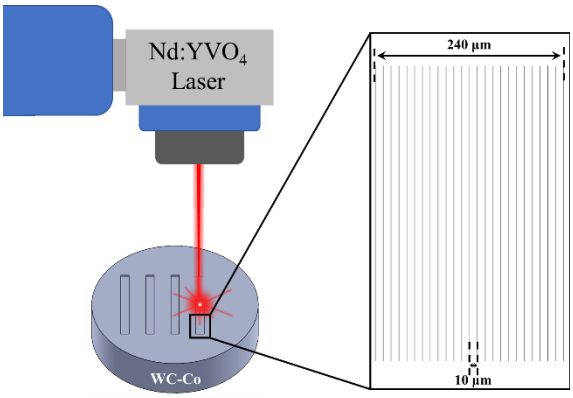

Figure 1. Schematic representation of the micro-grooves production process.

Table 1: Laser parameters combinations used for micro-grooves production.

Experiment	Laser power (W)	Scan speed (mm/s)	Pulse repetition rate (kHz)	Number of Passages
A	15	256	20	5
B				10
C				15
D				20
E				25
F				30
G				35
H				40
I				45
J				50

Additive manufacturing of embedded thermocouples

In order to manufacture the embedded type K and type N thermocouples in the WC-10wt.%Co substrates, a Multi-Material Laser Powder Bed Fusion (MMLPBF) system developed at the Center for MicroElectroMechanical Systems (CMEMS) at University of Minho was used [23,24]. This system is equipped with a Nd:YAG laser with a maximum working power of 80 W, multiple powder layer deposition functions and individually vacuum cleaning to avoid mixing of the different powders. During the fabrication, a building platform heated at 150 °C and an argon atmosphere to avoid the formation of oxides were used.

Thermocouple alloys powder, namely chromel, alumel, nicrosil and nisil, were produced by high-energy ball milling to be used in the LPBF process with a D50 particle size of 21.2 µm, 23.4 µm, 25.0 µm and 35.8 µm, respectively. SEM images of the high-energy ball milled thermocouple alloys powder are shown in Figure 2 and the chemical composition is presented in Table 2.

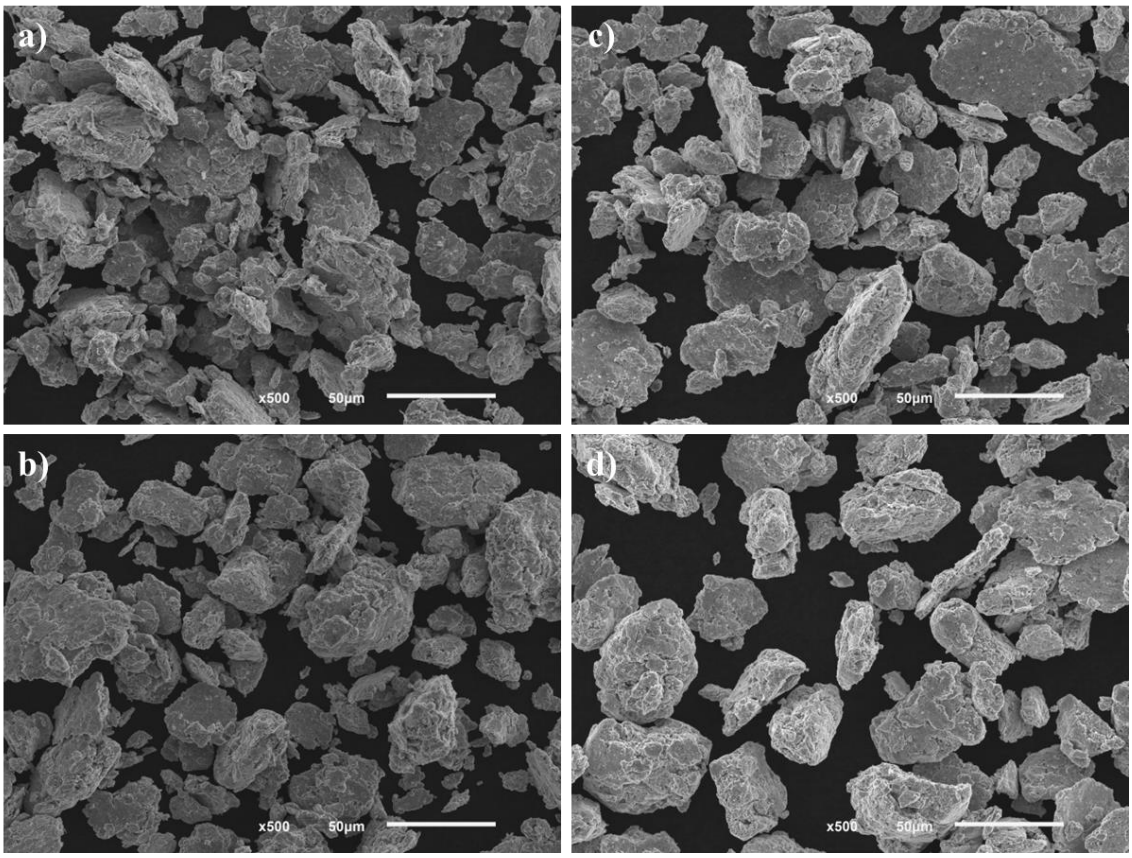

Figure 2. SEM images of the thermocouple alloys powder: a) chromel; b) alumel; c) nicrosil; d) nisil.

Table 2. Chemical composition of the thermocouple alloys powder.

Thermocouple	Material	Chemical composition (wt%)							
		Ni	Cr	Si	Al	Mn	Co	Mg	O
Type K	Chromel (+)	78.9	15.3	1.1	–	–	–	–	4.6
	Alumel (-)	88.9	–	2.4	1.5	1.5	0.5	–	5.3
Type N	Nicrosil (+)	72.1	21.4	2.3	–	–	–	–	4.2
	Nisil (-)	88.8	–	6.2	–	–	–	0.1	4.9

After some series of preliminary tests, a set of processing parameters was defined to be used in the LPBF process: laser power of 14.4 W, scan speed of 120 mm/min, pulse repetition rate of 12 Hz, pulse length of 0.5 ms and spot size of 400 µm. SEM was used to evaluate the produced embedded thermocouples and the composition at the interface between thermocouples positive and negative leg (hot junction) was assessed by Energy Dispersive X-Ray Spectroscopy (EDS).

The WC-10wt.%Co substrates embedded with the type K and type N thermocouples were then calibrated by using PREZYS T-25N equipment. For these tests, temperature was measured and compared against a reference (conventional) thermocouple, by heating from 20 to 120 °C and then cooling from 120 °C to 20

°C, at intervals of 20 °C with a stabilization time of 300 s for each step, being performed three tests for each thermocouple type embedded in different WC-10wt.%Co substrates.

RESULTS AND DISCUSSION

As previously mentioned, in this study several different combinations of parameters were tested to assess the optimum laser parameters for producing grooves with suitable dimensions for subsequent thermocouples alloys powder filling with particle size below 50 µm and production of embedded thermocouples by LPBF. SEM images of the micro-grooves cross-section, obtained accordingly to the set of experiments found in Table 1 are shown in Figure 3, being their dimensions presented in Table 3.

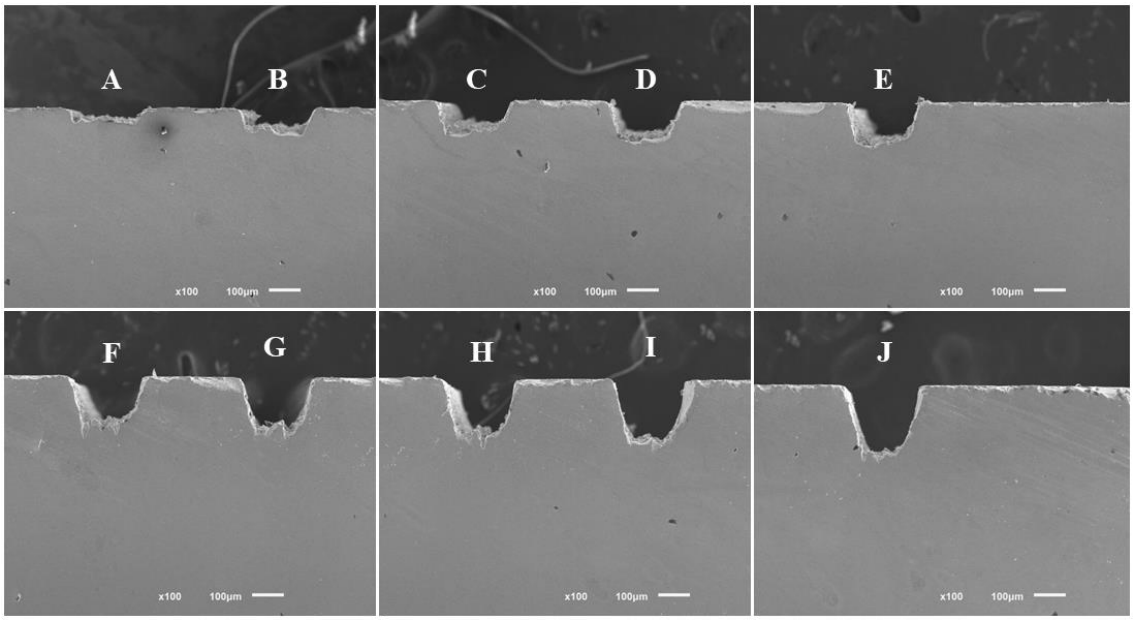

Figure 3. Cross-section SEM images of the micro-grooves produced using the set of experiments found in Table 1.

Table 3. Micro-grooves dimensions.

Experiment	Groove width (µm)	Groove depth (µm)
A	230.44 ± 1.75	42.56 ± 1.11
B	234.89 ± 5.87	85.36 ± 1.68
C	236.22 ± 5.59	95.16 ± 3.05
D	241.56 ± 1.91	123.20 ± 1.39
E	238.67 ± 0.54	127.48 ± 1.15
F	228.89 ± 1.13	142.35 ± 2.34
G	223.34 ± 1.96	154.51 ± 0.84
H	220.89 ± 2.06	184.91 ± 1.78
I	223.78 ± 0.83	193.46 ± 5.21
J	229.11 ± 1.26	218.69 ± 2.49

As shown in Figure 3, the employed strategy to achieve the desired micro-groove dimensions resulted in round-shaped grooves, due to the Gaussian energy distribution of the laser beam. This shape is potentially beneficial for the embedding process, since it doesn't contribute to the creation of stress concentration points, due to a more gradual transition along the groove depth. Additionally, the micro-groove shape

changes with the number of passages, i.e., for experiments F, G and H (30, 35 and 40 passages, respectively), the removal of material appears to be more difficult in the middle of the groove, leading to a flatter shaped micro-groove with a very rough surface. This phenomenon also happens for experiments A and B, since the low number of passages mitigates the contribution of the laser beam energy distribution to the micro-groove shape. As expected, the increase in the number of passages, resulted in an increase of micro-groove depth.

Furthermore, no microcracks, spatter, and heat-affected zones were observed, aspects that could compromise the integrity and mechanical strength of the WC-10wt.%Co substrates, allowing to conclude that the laser parameters for micro-grooves production were properly selected.

Regarding the micro-groove width, no significant differences were found, being the obtained values well aligned with the desired width. For experiments F, G and H, the less material removal in the middle of the groove, appears to influence the groove width. Considering the obtained results, laser processing parameters of experiment D, i.e., 20 passages, were selected for micro-groove production for subsequent thermocouples alloys powder filling and embedded thermocouples production by LPBF, since a micro-groove width of 241.56 ± 1.91 µm and depth of 123.20 ± 1.39 µm were obtained, being these dimensions well-aligned with the desired.

Figure 4 and Figure 5 show SEM images and EDS mapping at the thermocouple's hot junction for the type K and type N embedded thermocouples produced in the micro-groove designed for this purpose in the previous stage. To the authors best knowledge, the present study is the first reporting the possibility of using additive manufacturing technologies to produce embedded thermocouples in WC-Co cutting tools for cutting temperature measurement.

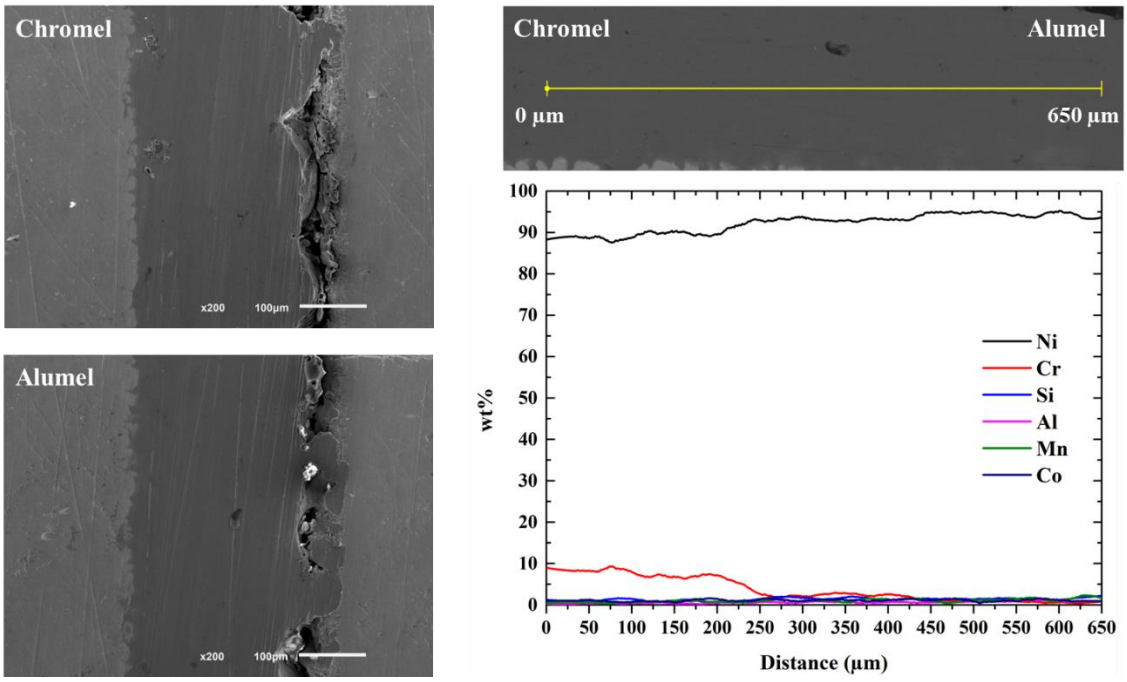

Figure 4: Type K SEM images and EDS mapping at the thermocouple hot junction.

It is possible to observe that the thermocouples surface is almost free of pores, thus indicating that the LPBF fabrication strategy and processing parameters were adequate to ensure the production of dense and continuous type K and type N embedded thermocouples, with no evidence of severe defects that can affect the thermocouples functionality. Also, the interface between thermocouples and WC-10wt.%Co substrate is clearly identifiable. However, the micro-groove is not completely filled due to being difficult

to ensure a precise positioning. Additionally, some micro-cracks are observed, mainly for nisil, probably due to the inherent rapid heating and cooling rates of this process and/or the difference in thermal properties of the thermocouples and substrate materials. When scanned by the laser, the heated layer expands but is restricted by the surrounding area, in this case, the WC-10wt.%Co substrate, which generates compressive stresses. On the other hand, when the laser moves away, cooling leads to contraction of the layer, that is however restricted by the surrounding area, leading to tensile stresses being accumulated, which results in high residual stresses and cracks formation at the interfacial zone [20,25].

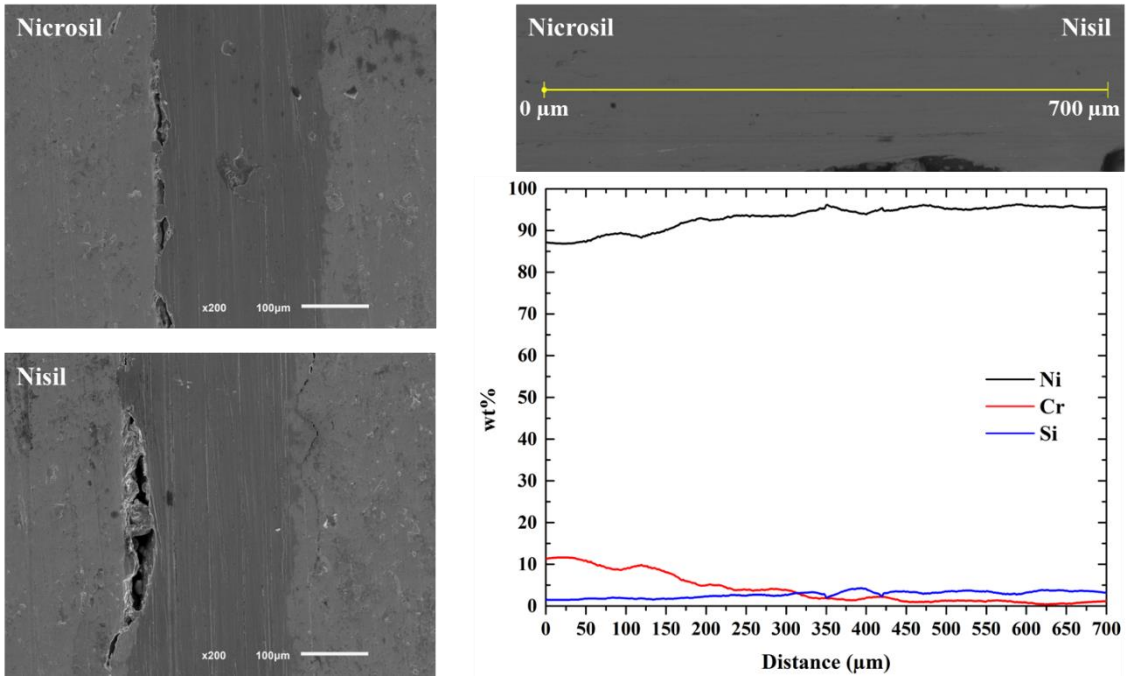

Figure 5: Type N SEM images and EDS mapping at the thermocouple hot junction.

EDS mapping results show that the hot junction formation was successfully achieved, since a transition between materials was found, despite SEM images not being able to show this outcome. As Ni is the main element in type K and type N thermocouple alloys, as presented in Table 2, the contrast between positive and negative leg is not evident. A gradual transition interface between the thermocouples positive and negative leg is clearly identifiable, tending its chemical composition to the theoretical value, which proves the feasibility of this approach to produce embedded thermocouples in WC-Co cutting tools.

Figure 6 depicts the temperature measured by the type K and type N embedded thermocouples in comparison with a reference thermocouple during the calibration test, being three tests performed for each thermocouple type in different WC-10wt.%Co substrates embedded with thermocouples.

Type K embedded thermocouple exhibit a very small deviation in the measured temperature in comparison with the reference thermocouple, with an average and maximum deviation of 0.75 °C and 1.20 °C, respectively, over the evaluated temperature range. Considering that a conventional thermocouple accuracy can be ± 2.5 °C, the measured temperature of the type K embedded thermocouple is in very good agreement with a conventional thermocouple. Regarding the type N embedded thermocouple, an average deviation of 11.55 °C and maximum deviation of 33.80 °C was found. This larger deviation may be explained by a possible greater sensitivity of type N thermocouple to electrical interferences with the substrate, due to the absence of an insulating layer between the thermocouple and WC-10wt.%Co substrate. Also, the greater particle size of nisil alloy may have some influence in this

outcome. However, since type N thermocouple presents a linear relationship with temperature, a reliable approximation to the real temperature can be made by correlation to the measured temperature by extrapolation. Despite these differences, for each thermocouple type the measurements showed repeatable results in all the performed calibration tests.

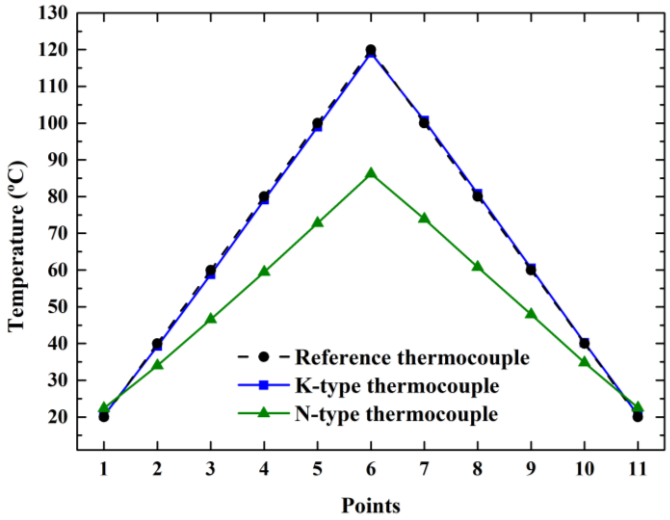

Figure 6. Calibration tests of the type K and type N embedded thermocouples.

CONCLUSIONS

- Laser surface modification was able to produce a micro-groove with the desired dimensions for subsequent thermocouple alloys powder filling and embedded thermocouple production by LPBF.
- The laser parameters used for micro-grooves production were properly selected, since no microcracks, spatter, or heat-affected zones were observed.
- The selected LPBF fabrication strategy and processing parameters were adequate to ensure the production of dense and continuous type K and type N embedded thermocouples with no evidence of severe defects.
- Complete filling of the micro-groove was not achieved, due to being difficult to ensure a precise positioning, and some micro-cracks were observed, probably due to the inherent rapid heating and cooling rates of this process and/or the difference in thermal properties of the thermocouples and substrate materials.
- EDS mapping results show that the hot junction formation was successfully achieved, since a gradual transition interface between materials was clearly identifiable.
- An average and maximum deviation of 0.75 °C and 1.20 °C, respectively, was found for type K embedded thermocouple in comparison with the reference thermocouple, while for the type N embedded thermocouple, an average deviation of 11.55 °C and maximum deviation of 33.80 °C was found.
- These results indicate that the proposed approach is suitable for additively manufacture embedded type K and type N thermocouples in WC-Co cutting tools by laser powder bed fusion for real time cutting temperature measurement, allowing an optimization of the cutting parameters during in-service time, thus enhancing tool performance and life.

Acknowledgements

This work was supported by FCT (Fundação para a Ciência e a Tecnologia) through the grant 2020.07155.BD and by the project POCI-01-0145-FEDER-030353 (SMARTCUT) and PTDC/EME-EME/1442/2020 (Add2MechBio). Additionally, this work was supported by FCT national funds, under the national support to R&D units grant, through the reference projects UIDB/04436/2020 and UIDP/04436/2020. Finally, this work was also developed within the scope of the project CICECO-Aveiro Institute of Materials, UIDB/50011/2020, UIDP/50011/2020 & LA/P/0006/2020, financed by national funds through the FCT/MCTES (PIDDAC).

REFERENCES

[1] E.M. Trent, P.K. Wright, Heat in metal cutting, in: Met. Cut., Fourth Edi, Butterworth-Heinemann, 2000: pp. 97–131.

[2] J. Zhao, Z. Liu, B. Wang, J. Hu, Y. Wan, Tool coating effects on cutting temperature during metal cutting processes: Comprehensive review and future research directions, Mech. Syst. Signal Process. 150 (2021) 107302. https://doi.org/10.1016/j.ymssp.2020.107302.

[3] N.A. Abukhshim, P.T. Mativenga, M.A. Sheikh, Heat generation and temperature prediction in metal cutting: A review and implications for high speed machining, Int. J. Mach. Tools Manuf. 46 (2006) 782–800. https://doi.org/10.1016/j.ijmachtools.2005.07.024.

[4] W. Grzesik, Heat in Metal Cutting, in: W. Grzesik (Ed.), Adv. Mach. Process. Met. Mater., Elsevier, 2017: pp. 163–182.

[5] N.L. Bhirud, R.R. Gawande, Measurement and prediction of cutting temperatures during dry milling: review and discussions, J. Brazilian Soc. Mech. Sci. Eng. 39 (2017) 5135–5158. https://doi.org/10.1007/s40430-017-0869-7.

[6] B. Guimarães, J. Rosas, C.M. Fernandes, D. Figueiredo, H. Lopes, O.C. Paiva, F.S. Silva, G. Miranda, Real-Time Cutting Temperature Measurement in Turning of AISI 1045 Steel through an Embedded Thermocouple — A Comparative Study with Infrared Thermography, J. Manuf. Mater. Process. 7 (2023) 50. https://doi.org/10.3390/jmmp7010050.

[7] P. Kovac, M. Gostimirovic, D. Rodic, B. Savkovic, Using the temperature method for the prediction of tool life in sustainable production, Measurement. 133 (2019) 320–327. https://doi.org/10.1016/j.measurement.2018.09.074.

[8] B.M. Pereira Guimarães, C.M. da Silva Fernandes, D. Amaral de Figueiredo, F.S. Correia Pereira da Silva, M.G. Macedo Miranda, Cutting temperature measurement and prediction in machining processes: comprehensive review and future perspectives, Int. J. Adv. Manuf. Technol. 120 (2022) 2849–2878. https://doi.org/10.1007/s00170-022-08957-z.

[9] R.F. Brito, S.R. Carvalho, S.M.M. Lima E Silva, Experimental investigation of thermal aspects in a cutting tool using comsol and inverse problem, Appl. Therm. Eng. 86 (2015) 60–68.

https://doi.org/10.1016/j.applthermaleng.2015.03.083.

[10] P. Childs, Thermocouples, in: P. Childs (Ed.), Pract. Temp. Meas., Butterworth-Heinemann, 2001: pp. 98–144.

[11] J. Rosas, H. Lopes, B. Guimarães, P.A.G. Piloto, G. Miranda, F.S. Silva, O.C. Paiva, Influence of Micro-Textures on Cutting Insert Heat Dissipation, Appl. Sci. 12 (2022) 6583. https://doi.org/ 10.3390/app12136583.

[12] RS Components, Thermocouple Selection Guide, 2018.

[13] P.B. Coates, The replacement of type K by nicrosil-nisil thermocouples, J. Phys. E. 14 (1981) 1246–1247. https://doi.org/ 10.1088/0022-3735/14/11/005.

[14] A.R. Samboruk, A.P. Amosov, E.A. Kuznets, A.A. Kuzina, Y.M. Markov, Development of technology of Nicrosil and nisil thermocouple materials using extrusion of metal powders, Key Eng. Mater. 746 KEM (2017) 201–206. https://doi.org/10.4028/www.scientific.net/KEM.746.201.

[15] M.W. Hastings, J.. V. Pearce, G. Machin, Electrical resistance breakdown of type N mineral-insulated metal-sheathed thermocouples above 800°C, Meas. Tech. 55 (2012) 60–63.

[16] S. Chowdhury, N. Yadaiah, C. Prakash, S. Ramakrishna, S. Dixit, L.R. Gupta, D. Buddhi, Laser powder bed fusion: a state-of-the-art review of the technology, materials, properties & defects, and numerical modelling, J. Mater. Res. Technol. 20 (2022) 2109–2172. https://doi.org/10.1016/j.jmrt.2022.07.121.

[17] P. M., Additive Manufacturing of Tungsten Carbide Hardmetal Parts by Selective Laser Melting (SLM), Selective Laser Sintering (SLS) and Binder Jet 3D Printing (BJ3DP) Techniques, Lasers Manuf. Mater. Process. 7 (2020) 338–371. https://doi.org/10.1007/s40516-020-00124-0.

[18] P. Bidare, A. Jiménez, H. Hassanin, K. Essa, Porosity, cracks, and mechanical properties of additively manufactured tooling alloys: a review, Adv. Manuf. 10 (2022) 175–204. https://doi.org/10.1007/s40436-021-00365-y.

[19] C. Singer, M. Schmitt, G. Schlick, J. Schilp, Multi-material additive manufacturing of thermocouples by laser-based powder bed fusion, Procedia CIRP. 112 (2022) 346–351. https://doi.org/10.1016/j.procir.2022.09.007.

[20] B. Guimarães, A. Guedes, C.M. Fernandes, D. Figueiredo, F. Bartolomeu, G. Miranda, F.S. Silva, WC-Co/316L stainless steel joining by laser powder bed fusion for multi-material cutting tools manufacturing, Int. J. Refract. Met. Hard Mater. 112 (2023) 106140. https://doi.org/10.1016/j.ijrmhm.2023.106140.

[21] J. García, V. Collado Ciprés, A. Blomqvist, B. Kaplan, Cemented carbide microstructures: a review, Int. J. Refract. Met. Hard Mater. 80 (2019) 40–68. https://doi.org/10.1016/j.ijrmhm.2018.12.004.

[22] B. Guimarães, J. Silva, C.M. Fernandes, D. Figueiredo, O. Carvalho, G. Miranda, F.S. Silva, Understanding drop spreading behaviour on WC-10wt%Co cutting tools – an experimental and numerical study, Colloids Surfaces A Physicochem. Eng. Asp. 637 (2022) 128268. https://doi.org/10.1016/j.colsurfa.2022.128268.

[23] F. Bartolomeu, O. Carvalho, M. Gasik, F.S. Silva, Multi-functional Ti6Al4V-CoCrMo implants fabricated by multi-material laser powder bed fusion technology: A disruptive material's design and manufacturing philosophy, J. Mech. Behav. Biomed. Mater. 138 (2023) 105583. https://doi.org/10.1016/j.jmbbm.2022.105583.

[24] A. Cunha, A. Marques, F.S. Silva, M. Gasik, B. Trindade, O. Carvalho, F. Bartolomeu, 420 stainless steel-Cu parts fabricated using 3D Multi-Material Laser Powder Bed Fusion: a new solution for plastic injection moulds, Mater. Today Commun. 32 (2022) 103852. https://doi.org/10.1016/j.mtcomm.2022.103852.

[25] C.G. Moura, O. Carvalho, V.H. Magalhães, R.S.F. Pereira, M.F. Cerqueira, L.M.V. Gonçalves, R.M. Nascimento, F.S. Silva, Laser printing of micro-electronic communication systems for smart implants applications, Opt. Laser Technol. 128 (2020) 106211. https://doi.org/10.1016/j.optlastec.2020.106211.